Development of a Strong Beam Guardrail-to-Bridge-Rail Transition

ROGER P. BLIGH, DEAN L. SICKING, AND HAYES E. ROSS, JR.

This study describes the development and testing of a strong beam guardrail-to-bridge-rail transition. Barrier VII was validated and used to simulate impacts with flexible barriers attached to a rigid barrier. Design curves for selecting transition design parameters of beam strength, post size, and post spacing are presented. The selected design incorporated a tubular W-beam rail element mounted on 7-inch round posts spaced on 3-foot, 1.5-inch centers. The transition was designed to simplify retrofit operations and can be used on bridges that require bridge-end drains. Three full-scale crash tests were conducted to verify the acceptable performance of the transition when attached to either a vertical concrete parapet or a concrete safety-shaped barrier.

A bridge rail is a longitudinal barrier to prevent errant vehicles from going over the side of a bridge. Because of their critical nature, most bridge rails are either rigid or semi-rigid so they can limit dynamic deflections and safely contain a vehicle without allowing it to extend beyond the edge of the bridge deck. Two common types of bridge rails are reinforced concrete safety-shaped barriers and vertical concrete parapets. The exposed ends of these rigid concrete barriers can pose a serious safety hazard. Safety can be increased with approach roadside barriers. Approach roadside barriers are warranted not only to shield the exposed bridge rail end but also to prevent errant vehicles from getting behind the railing and falling off the bridge. These approach barriers are typically much more flexible than the bridge rails or wingwalls to which they are attached. Flexible barriers can deflect sufficiently to allow an errant vehicle to impact or "snag" on the end of the rigid barrier, even when the two barriers are securely attached. Therefore, a transition section is required whenever there is a significant change in lateral strength from the approach barrier to the bridge rail. The transition section should provide a smooth change in lateral barrier stiffness to prevent impacting vehicles from snagging on the end of the rigid barrier.

Strong post W-beam guardrail is the most common bridge approach railing in use today. Most existing transitions involve reducing guardrail post spacing to 3 feet, 1.5 inches near the end of the bridge rail. This transition design is unable to prevent severe snagging on the end of rigid concrete barriers (*1*). Several acceptable guardrail-to-bridge-rail transition designs using 1-foot, 6.75-inch post spacings and rub rails near the bridge end have been developed by Bronstad (*1*). Although these designs exhibit good impact performance, the tight post spacing presents a problem when used on bridges designed to drain water around the end of the railing. The maximum distance between posts in these designs is only 12 inches—inadequate for most bridge end drain designs. Drainage problems are especially acute when the new transitions are used to retrofit existing bridge sites. Other acceptable transition designs were developed by Post and presented at the meeting of TRB's Committee on Roadside Safety Features in January 1987. These systems are characterized by oversized posts, reduced post spacing near the bridge end, nested W-beam or thrie-beam rails, and flared bridge rail ends. Problems associated with implementing these designs include inventory and repair problems arising from the use of nonstandard guardrail post and the high costs of flaring bridge rail ends during retrofit operations.

In view of the general lack of acceptable guardrail-to-bridge-rail transitions that can be economically implemented in retrofit situations, this study was undertaken to develop a new transition design with the following characteristics:

1. Provide for easy retrofit of existing installations.
2. Provide sufficient post spacing to allow implementation where bridge-end drains are required.
3. Design transitions for use with either vertical concrete parapets or concrete safety shaped barriers.
4. Meet nationally recognized safety standards.

RESEARCH APPROACH

As mentioned previously, a guardrail-to-bridge-rail transition must be designed to prevent impacting vehicles from deflecting the guardrail sufficiently to allow vehicle snagging on the end of the stiffer barrier. Standards for testing barrier transitions are presented in NCHRP Report 230 (*2*). This report requires that transitions be evaluated with a single test that involves a vehicle impacting the more flexible barrier upstream from its transition to the stiffer barrier. This test condition examines the propensity for the flexible barrier to deflect and allow the test vehicle to snag on the end of the rigid barrier. The size of the test vehicle and impact speed and angle vary with the level of service of the barrier system (*2*). Most concrete bridge rails and strong-post guardrail systems have been tested to service level 2 as described in NCHRP Report 230. For service level 2, NCHRP Report 230 requires that transitions be tested with a 4,500-pound automobile, impacting at 60 miles per hour and 25 degrees. Note that in most practical guardrail-to-bridge-rail transition designs the guardrail is first transitioned into an intermediate strength barrier that is then

Texas Transportation Institute, Texas A&M University System, College Station, Tex. 77843

TABLE 1 POST PARAMETERS FOR BARRIER VII INPUT

MATERIAL	WOOD	WOOD	STEEL
SIZE	6" X 8" (1)	7" DIAM. (7)	W6 X 8.5 (1)
k_A (k/in.)	1.95	2.9	1.15
k_B (k/in.)	1.56	2.9	2.46
M_A (in-k)	191.1	256.	256.2
M_B (in-k)	214.2	256.	107.1
F_A (k)	10.2	12.2	5.1
F_B (k)	9.1	12.2	12.2
Δ_A (in.)	4.7	18.	13.6
Δ_B (in.)	15.5	18.	13.2

(Effective Rail Height = 21")

A – Denotes Longitudinal or Major Axis

B – Denotes Transverse or Minor Axis

k – Stiffness of Post For Elastic Horizontal Deflections

M – Base Moment At Which Post Yields

F – Shear Force Causing Failure of Post

Δ – Deflection Causing Failure of Post

transitioned into the rigid bridge rail. Safety performance of the design must be evaluated at both transition points.

The Barrier VII simulation model (*3*) is capable of accurately predicting barrier deflections for impacts involving full-size vehicles impacting at speeds up to 60 miles per hour and angles up to 25 degrees (*4, 5*). Further, for impacts into barriers placed on flat terrain, such as that found on the approach to a bridge, vehicle vaulting, override, and underride is of little concern. Thus the 2-D nature of the Barrier VII program was not considered to be a severe limitation and this model was chosen for use in developing the new transition design.

Although Barrier VII has been successfully used to simulate impacts with a variety of flexible barriers, its use in studying impacts near the transition from a flexible to a rigid barrier has been somewhat limited. Therefore the first step in transition development was to conduct a limited validation of Barrier VII for analysis of impacts in the region of a transition. Two full-scale crash tests of guardrail-to-bridge-rail transitions were selected from Bronstad et al. (*1*) for the validation effort. Simulated guardrail beam elements were assumed to be of uniform cross section and to have bilinear elastic/perfectly plastic properties both flexurally and extensionally. Simulated beam stiffness characteristics were estimated to be approximately 1.5 times calculated static values. Table 1 shows simulated post properties collected from Bronstad et al., Calcote, and Dewey et al. (*1, 6, 7*).

Since barrier deflection is the primary indicator of the propensity for a vehicle to snag on the concrete barrier, this parameter was selected as the primary measure of correlation between simulation and crash testing. As shown in Table 2, Barrier VII was found to give very good predictions of maximum barrier deflections for the two tests simulated. Other measures of simulation validity, including vehicle trajectory and crush, also showed excellent correlation between Barrier VII and the two crash tests.

The critical impact point for testing guardrail-to-bridge-rail transitions is the point at which the potential for snagging on the end of the rigid barrier is maximized. Note that this critical impact point changes with the stiffness of the approach barrier. Stiff approach barriers redirect impacting vehicles more quickly and therefore have a critical impact point nearer to the rigid barrier than more flexible approach rails. Bronstad (*1*) determined that for double W-beam rails mounted on posts spaced 1 foot, 6.75 inches apart, the critical impact point was approximately 112 inches upstream of the rigid barrier. Barrier VII simulations indicated that the critical impact location is the same for approach barriers that deflect approximately the same as those used in the study by Bronstad (*1*). Therefore this impact location was used for all simulation and testing of transitions to rigid barriers. Further, Barrier VII analysis indicated that the critical impact location on standard strong post guardrails is approximately 125 inches from the end of the intermediate barrier. Therefore, analysis and testing of impacts on standard guardrails was conducted using an impact point 125 inches upstream from the start of the transition.

Barrier VII was used to conduct a parameter study of designs for transitions to rigid barriers. All simulations involved impacts with a 4,500-pound vehicle traveling 60 miles per hour and

TABLE 2 BARRIER VII CRASH TEST SIMULATIONS

TEST NO.	DESCRIPTION	CONCRETE WINGWALL	IMPACT DATA LB/MPH/DEG	IMPACT POINT FROM WINGWALL	MAXIMUM LATERAL DEFLECTION ACTUAL	SIMULATED	% DIFF
T-1 (1)	THRIE BEAM BRIDGE TRANSITION	STRAIGHT	4658/61.5/25.2	96.5"	9.4"	9.92"	5.5
T-2 (1)	THRIE BEAM BRIDGE TRANSITION	TAPERED w/ WOOD BLOCK OUT	4650/64.0/25.6	112.5"	14.4"	14.74"	2.4

contacting the rail 112 inches upstream of the rigid barrier end at an angle of 25 degrees. The basic transition design consisted of a standard strong-post W-beam approach rail with modified post spacing and beam strength over the last 25 feet before the bridge rail. The bridge rail was modeled as a straight vertical concrete parapet. Design parameters investigated include beam strength, post spacing, and post size. The two post sizes investigated were a standard 7-inch diameter wood post and a "double strength" post. A double strength post was defined as a post that would develop twice the dynamic lateral resistance of the standard post. This can be achieved by increasing the post section modulus and either embedment depth or post width. Examples of double strength posts are an 8-inch × 8-inch wood post embedded approximately 48 inches and a 10-inch × 10-inch wood post embedded 40 inches. Figures 1 and 2 show predicted deflections for the two different post sizes studied. These figures were used to determine the barrier deflection that could be expected for a wide range of beam strengths and post spacings. Note that 6-inch × 8-inch wood posts and W 6 × 9 steel posts have dynamic lateral capacity similar to 7-inch diameter round wood posts. Thus, although figure 1 was developed for a 7-inch round post, either of these other posts could be substituted as the deflectors.

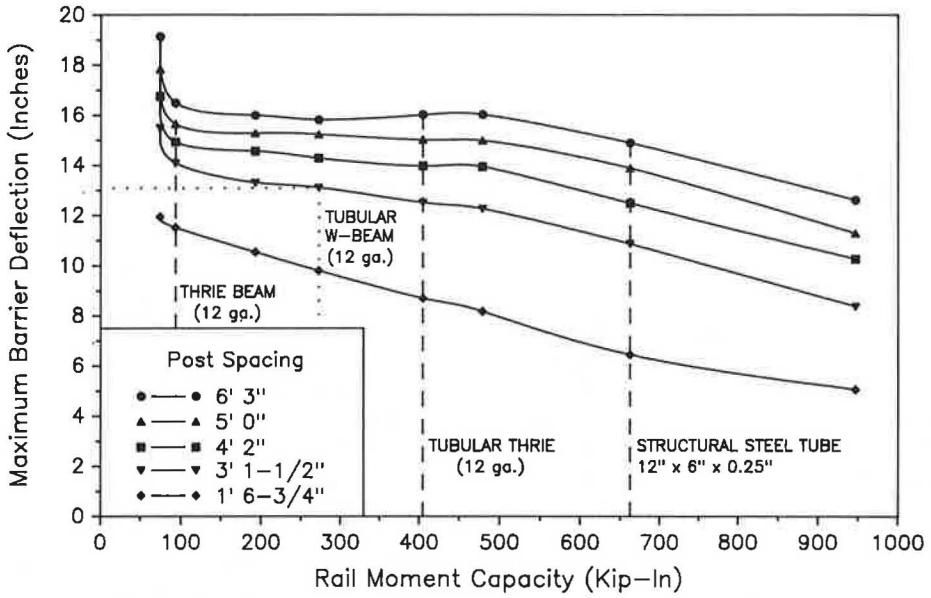

FIGURE 1 Design curves for standard post transitions.

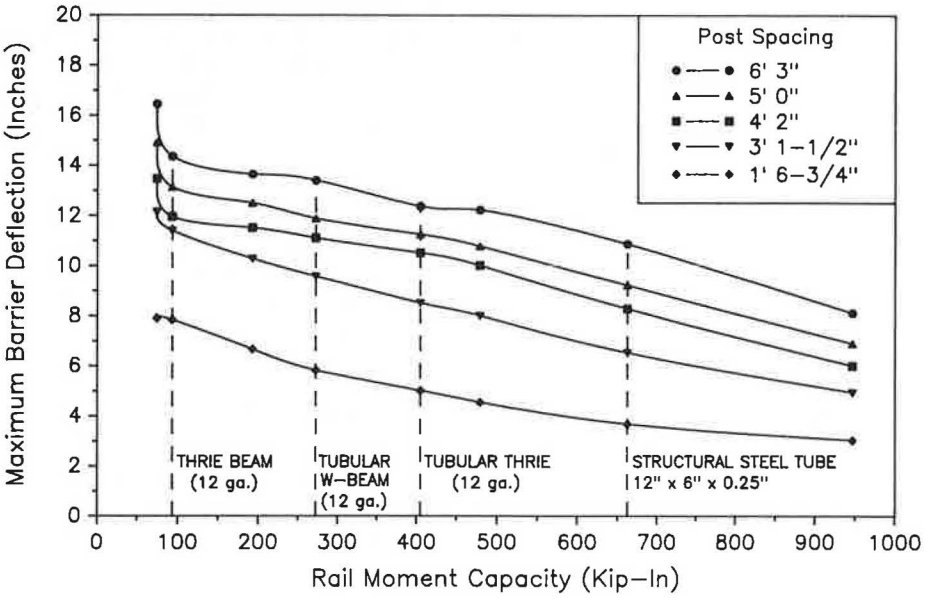

FIGURE 2 Design curves for double strength post transitions.

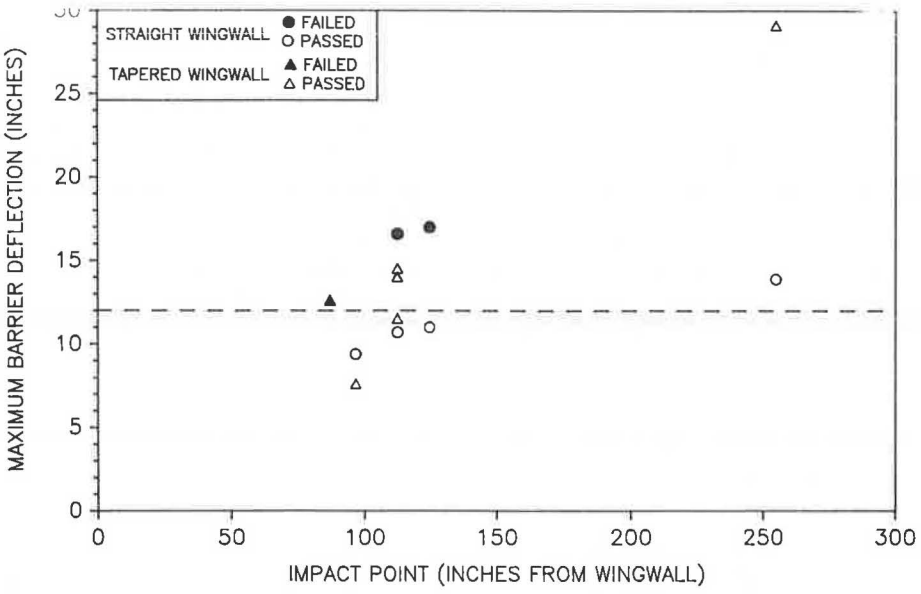

FIGURE 3 Maximum deflection from transition crash tests (*1*).

DEFLECTION LIMIT DESIGN CRITERIA

As discussed above, barrier deflection is believed to be a good indicator of the probability of a vehicle snagging on the end of a rigid barrier. Twelve full-scale crash tests taken from Bronstad et al. (*1*) were reviewed in an effort to determine the maximum allowable barrier deflection. Figure 3 shows barrier deflection for each of the tests conducted in the referenced study. As shown in Figure 3, for unflared bridge rail ends, the approach guardrail can be allowed to deflect no more than 12 inches before significant vehicle snagging becomes a potential problem. In support of the crash test data, a series of simulation runs were made to track wheel position past the end of the rigid barrier end. It was observed that for deflections in excess of 12 inches, the wheel followed a trajectory through the end of the concrete barrier, indicative of severe vehicle snagging and poor safety performance for the transition. However, for barrier deflections less than 12 inches the wheel followed a path safely outside of the bridge rail end. These results supported a deflection limit of 12 inches as the initial evaluation criteria in the transition design. It was concluded that all transition designs limiting maximum lateral deflections to less than 12 inches should provide acceptable performance.

SELECTION OF TRANSITION SYSTEM

Using Figures 1 and 2, a basic design is selected by choosing the type of post to be used (i.e., standard or strong) and either the post spacing or beam type desired. The remaining parameter is then found using the 12-inch deflection limit discussed above. For example, if it is desirable to maintain a 6-foot, 3-inch post spacing, a transition design would involve a beam with a yield moment of 660-kip-inch (such as a 12-inch × 6-inch × 0.25-inch structural steel tube) mounted on strong posts. This system has a predicted maximum barrier deflection of approximately 11 inches (see Figure 2). Similarly, if it is desirable to use a nested thrie beam (My = 190 kip-in.) in the transition zone, one alternative would be to mount it on "strong" posts spaced at 3 feet, 1.5 inches. This transition configuration has a predicted dynamic deflection of approximately 10.5 inches (see Figure 2).

As can be seen from Figures 1 and 2, numerous transition configurations were acceptable based on the 12-inch deflection limit criteria. Additional selection guidelines were established to aid in the determination of a final design. The transition should (1) be able to retrofit existing bridge rails, (2) provide sufficient post spacing to allow for adequate bridge end drainage, (3) allow for ease of transition at both approach rail and bridge rail, and (4) use standard hardware items.

Consultations with officials from the Texas State Department of Highways and Public Transportation (SDHPT) indicated that, because of inventory and maintenance problems associated with nonstandard guardrail posts, the new transition should be constructed with standard guardrail posts. Further, SDHPT engineers expressed an interest in developing a transition that used a 12 gauge tubular W-beam rail. This beam has an approximate moment capacity of 280 kip-inches. As shown in Figure 1, Barrier VII predicts a maximum deflection of 13 inches for the tubular W-beam mounted on standard posts spaced 3 feet, 1.5 inches. Although the predicted deflection for this design is slightly above the deflection limit criteria, it was believed that the added depth of tubular W-beam would act as an effective blockout. Thereby, effective deflection of the beam would be reduced to 10 inches, which is well below the deflection limit of 12 inches.

TRANSITION DESIGN

The final transition design consisted of a 25-foot segment of 12 gauge tubular W-beam mounted on 7-inch diameter round wood posts spaced 3 feet, 1.5 inches apart with a 38 inch embedment as shown in Figure 4. In an effort to identify other potential snagging problems and to determine the necessary connection design loadings, Barrier VII was then used

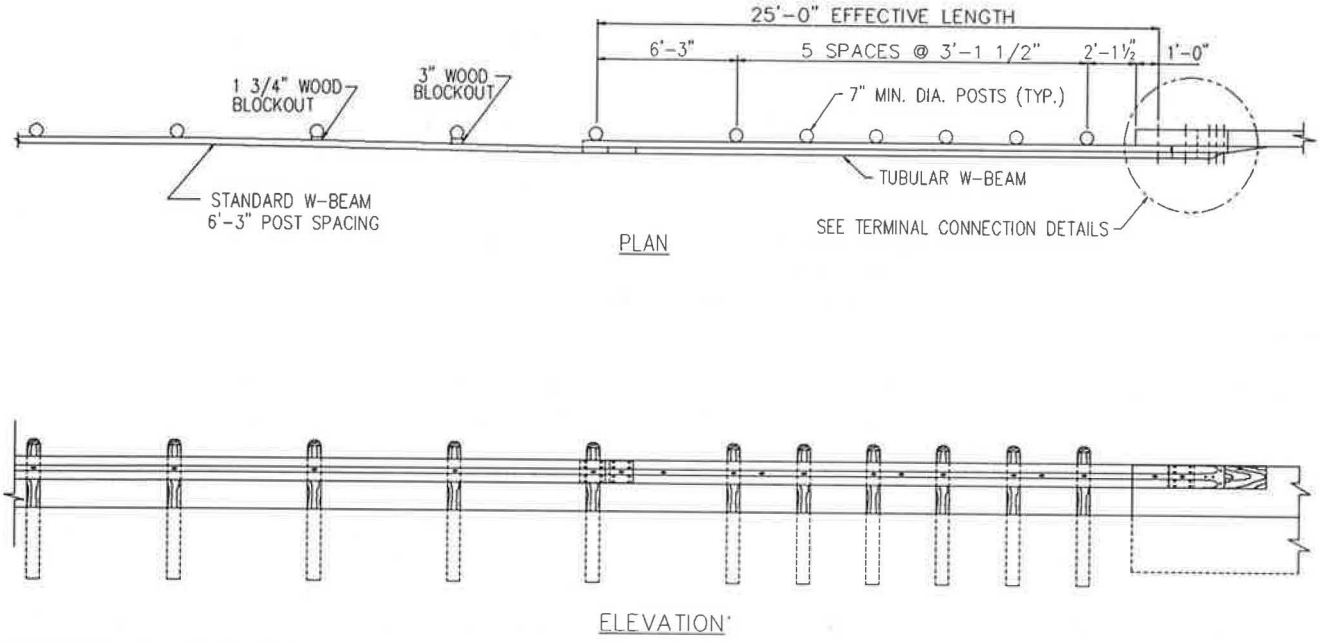

FIGURE 4 Guardrail-to-bridge-rail transition, retrofit design.

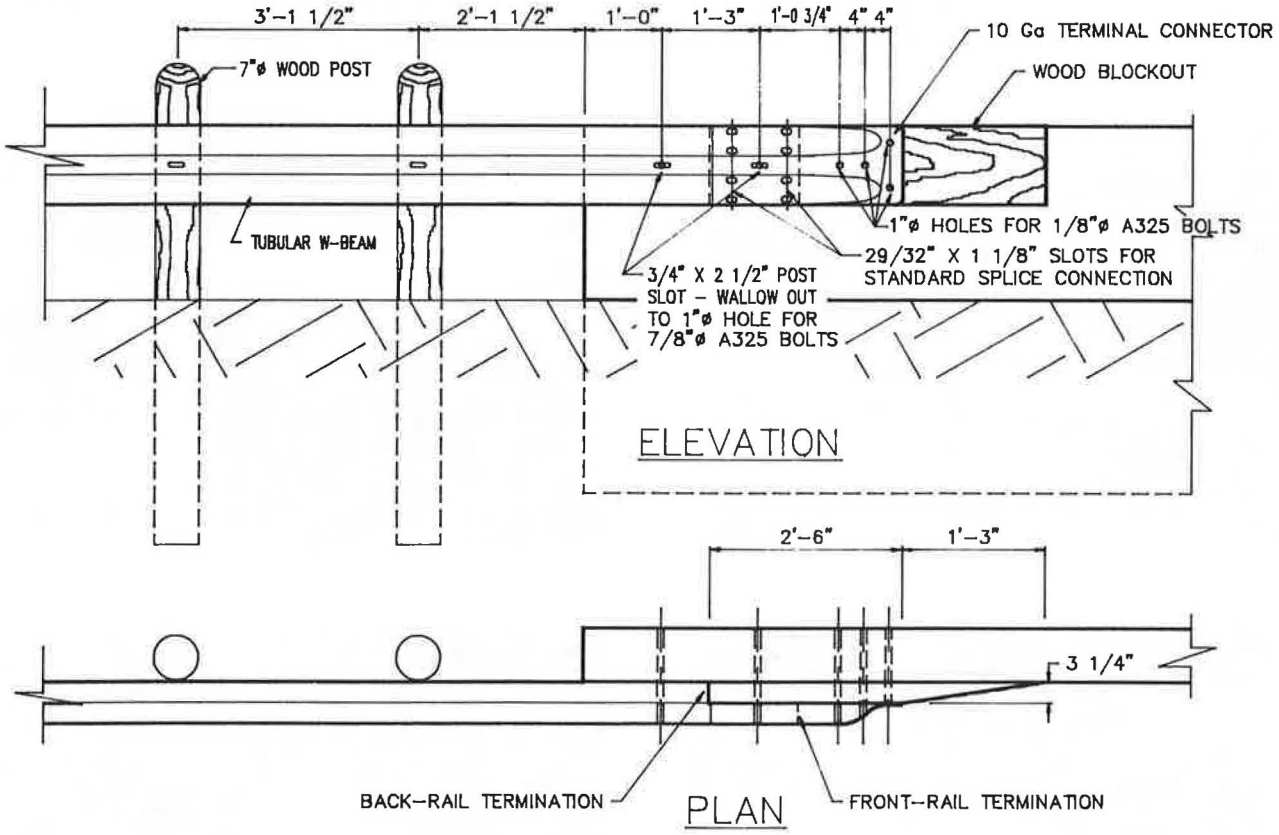

FIGURE 5 Terminal connection details.

to simulate impacts with the selected design at a number of locations. Barrier VII predicted that for impacts on the upstream transition from the single W-beam to the tubular W-beam, the possibility of wheel snagging would be reduced if the first post spacing on the tubular segment was maintained at 6-foot, 3-inch Design loading conditions from Barrier VII for the connection between the tubular W-beam and the concrete barrier end included a 140-kip tensile force, a 60-kip shear force, and a 280-kip-in. bending moment. This connection was accomplished with six ⅞-inch diameter high strength bolts (A325 or equivalent grade threaded rod), a steel end shoe, and a tapered wood blockout as shown in Figure 5. The connection was designed to be used with either vertical parapets or concrete safety-shaped barriers.

Note that the design shown in Figure 4 is a retrofit of the existing Texas standard transition and uses two small wood blockouts on the standard W-beam approach in order to move the rail to the outside of the tubular beam. No blocks were used in the rest of the transition to maintain compatibility with the Texas standard guardrail. Further, due to retrofit considerations, the attachment between the single W-beam barrier and the tubular W-beam rail required a small splice plate. Retrofitting an existing installation thus involves replacing a 25-foot length of W-beam railing, drilling six holes in the concrete barrier, and placing two small blockouts in the approach rail. In addition, an analysis of the bridge rail end should be made to ensure adequate strength and anchorage for carrying the increased impact forces transmitted by a strong beam transition because a strong beam barrier system is capable of transferring more shear and moment to the bridge rail end than the common flexible W-beam guardrail.

FULL-SCALE CRASH TESTS

The tubular W-beam transition was evaluated for impact performance in accordance with Test Number 30 of NCHRP Report 230 (*2*). Test 30 involves a 4,500-pound vehicle impacting the transition section at 60 miles per hour at an angle of 25 degrees. The testing program consisted of three full-scale crash tests, each of which evaluated a different aspect of the transition design. The tests conducted were as follows:

1. Evaluation of tubular W-beam transitioning into a vertical concrete parapet.
2. Evaluation of tubular W-beam transitioning into a concrete safety-shaped barrier.
3. Evaluation of the standard W-beam guardrail transitioning to the tubular W-beam.

Test 1

This test evaluated the tubular W-beam transition to a vertical concrete wall. The barrier transition was constructed as shown in Figure 4. Figure 6 shows the completed installation before Test 1.

A 4,570-pound Cadillac impacted the transition at 55 miles per hour and 26.4 degrees at a point 112 inches upstream from the bridge rail end. The vehicle was successfully redirected although significant wheel snagging on the bridge rail end was observed. Some sheet metal snagging occurred at the tops of the posts and minor wheel snagging occurred at the base of the posts. While the top of the tubular rail was only partially flattened, the bottom half of the rail was completely collapsed. This collapse effectively increased the maximum deflection of the rail and thus the degree of snagging. The test vehicle was

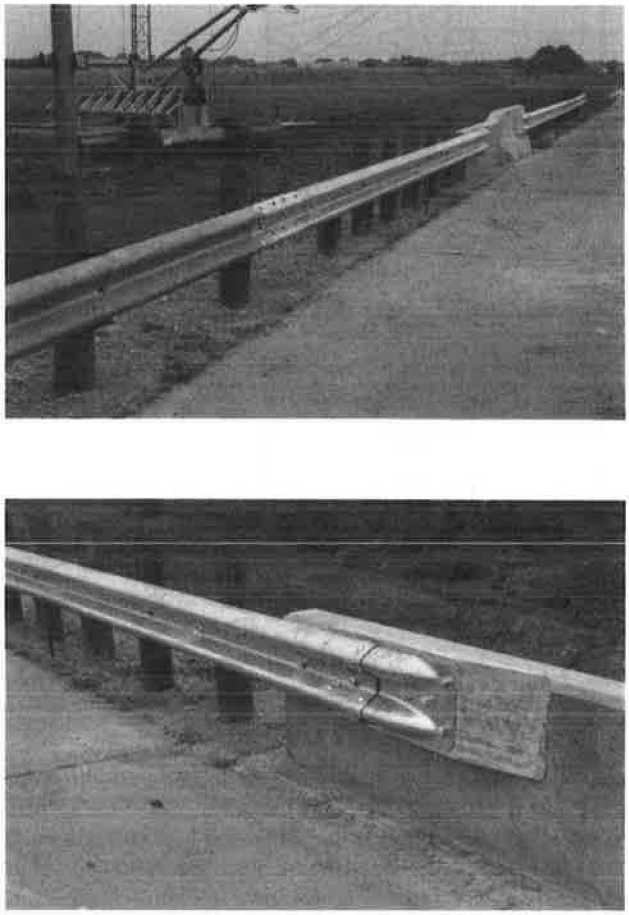

FIGURE 6 Tubular W-beam transition to vertical wall, Test 1 installation.

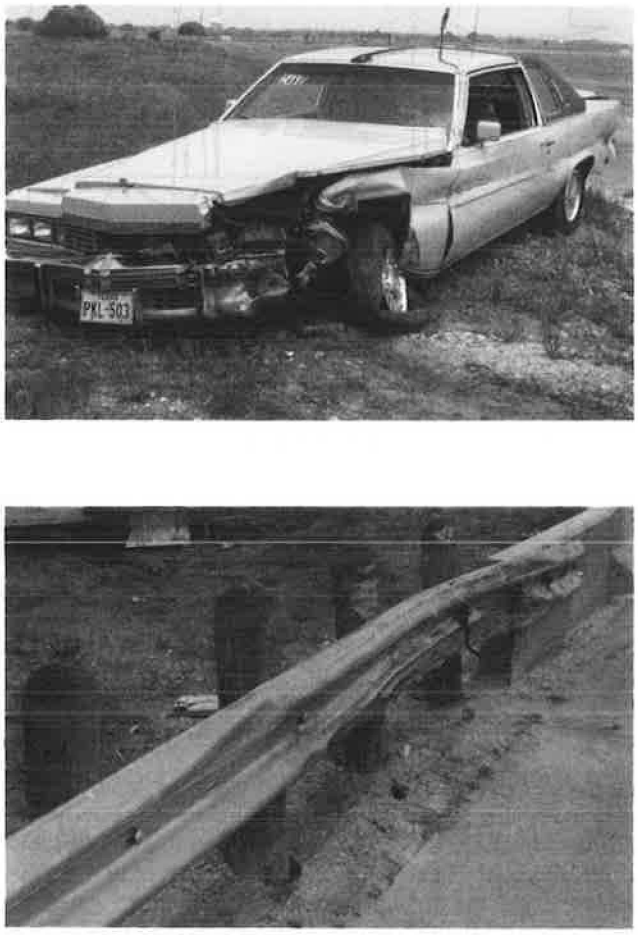

FIGURE 7 Vehicle and barrier damage after Test 1.

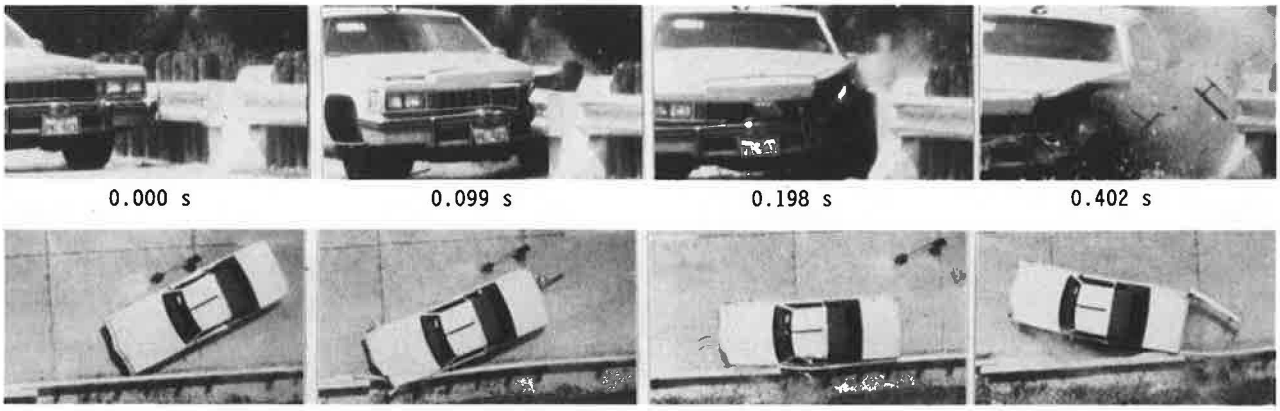

Test No	2461-1
Date	5/14/87
Test Installation	Tubular W-Beam Transition to T201
Length of Transition	25 ft (7.6 m)
Vehicle	1977 Cadillac
Vehicle Weight	
Test Inertia	4400 lb (1998 kg)
Gross Static	4570 lb (2075 kg)
Vehicle Damage Classification	
TAD	11LFQ6
CEC	11LFES4
Maximum Vehicle Crush	13.0 in (33.0 cm)
Max. Dyn. Rail Deflection	9.6 in (24.4 cm)
Max. Perm. Rail Deformation	4.8 in (12.2 cm)
Impact Speed	55.0 mi/h (88.5 km/h)
Impact Angle	26.4 deg
Exit Speed	33.1 mi/h (53.3 km/h)
Exit Angle	13.4 deg
Vehicle Accelerations (Max. 0.050-sec Avg)	
Longitudinal	-8.0 g
Lateral	-9.4 g
Occupant Impact Velocity	
Longitudinal	26.7 ft/s (8.1 m/s)
Lateral	22.0 ft/s (10.0 m/s)
Occupant Ridedown Accelerations	
Longitudinal	-3.1 g
Lateral	-11.5 g

FIGURE 8 Summary of results for Test 1.

only moderately damaged, considering the severity of the test. Damage to both the vehicle and barrier after Test 1 are shown in Figure 7. Note that hood snagging on the top of the wood posts and the concrete barrier was not considered to be a significant hazard since the hood rides up the post or barrier until it slips off of the top. There was no tendency for the hood to become detached from its hinges and penetrate the occupant compartment.

NCHRP Report 230 (*2*) does not require that a strength test such as that used for evaluation of transition designs meet occupant severity limits. However, the occupant severity measures from Test 1 were all within maximum acceptable limits. A summary of the test results is given in Figure 8.

Although the change in vehicle velocity was above the recommended value set forth in NCHRP 230 Evaluation Criteria I (*2*), this test was considered to be a success as presented in Discussion of Results.

Test 2

This test evaluated the tubular W-beam transition to the concrete safety-shaped barrier. The geometry of the safety-shaped rail increases the potential for vehicle snagging. The lower curb face of the barrier projects beyond the face of the tubular W-beam and the 32-inch wall height extends above the approaching guardrail. Some modifications were made to reduce the severity of snagging observed in Test 1. Wood inserts were added in both the top and bottom of the tubular W-beam to prevent the rail from collapsing (see Figure 9). Also, the tops of the posts were cut at rail height with a 10-degree bevel to minimize sheet metal snagging. Figure 10 shows the modified transition before Test 2.

A 4,637 pound Cadillac impacted the transition at 60.8 miles per hour and 25.8 degrees at a point 112 inches upstream from the bridge rail end. The vehicle was smoothly redirected with

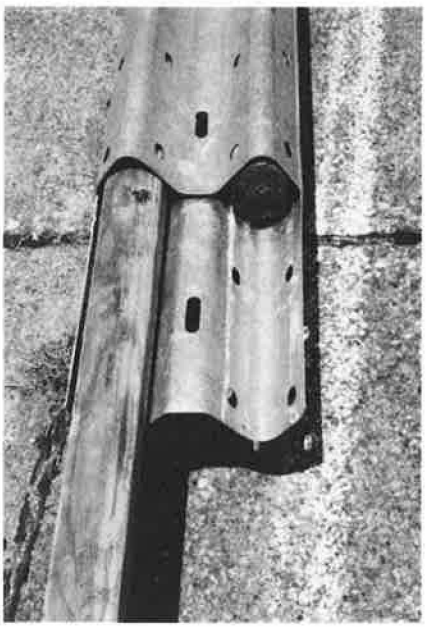

FIGURE 9 Wood inserts for tubular W-beam.

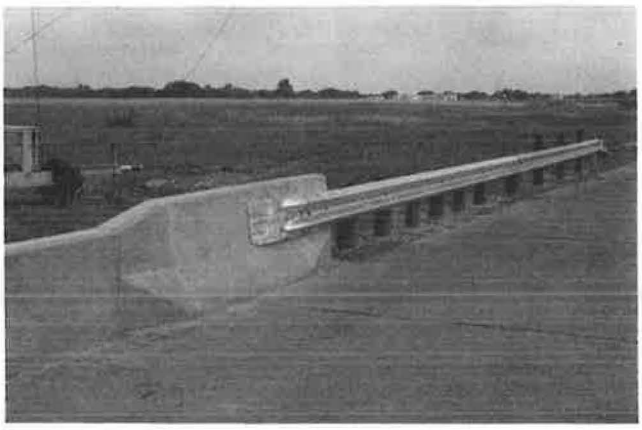

FIGURE 10 Tubular W-beam transition to CSSB, Test 2 installation.

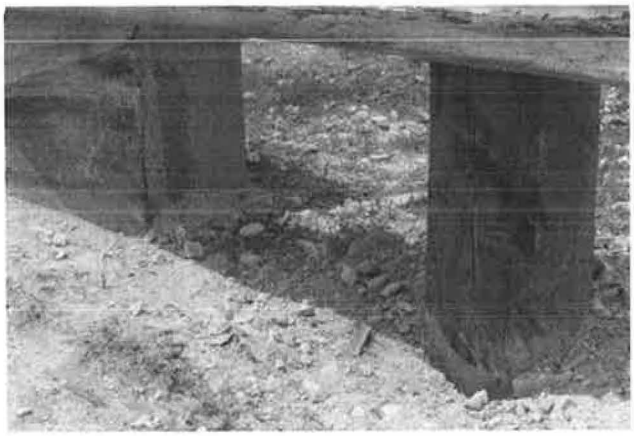

FIGURE 11 Evidence of snagging on posts and concrete wall.

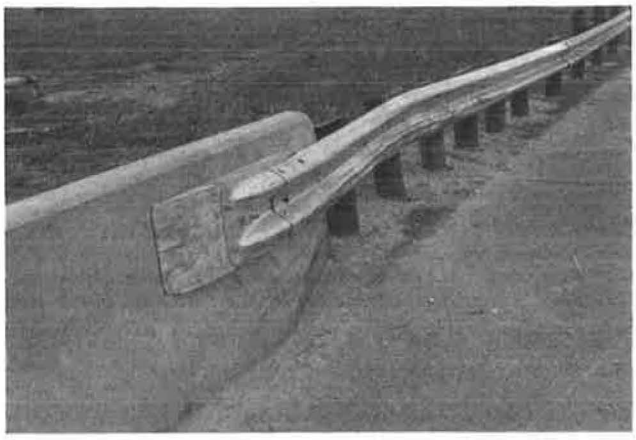

FIGURE 12 Vehicle and barrier damage after Test 2.

greatly improved performance over Test 1. The wood inserts prevented the tubular rail from collapsing and greatly reduced the degree of snagging. Minor wheel snagging was observed at the base of posts 1 and 2 and at the bridge rail end. Although some sheet metal snagging occurred on the top of the concrete rail, the forces involved appeared to be significantly lower than in the previous test. Evidence of the post and wingwall snagging is shown in Figure 11.

The vehicle damage sustained in Test 2 was moderate for the severity of the impact. Damage to the vehicle and barrier after Test 2 is shown in Figure 12. Although not a requirement for the transition test, the occupant impact indexes of NCHRP Report 230 (2) were all within maximum acceptable limits. A summary of Test 2 results is given in Figure 13.

Test 3

This test evaluated the performance of the W-beam transition to the tubular W-beam. The guardrail was not blocked out for this test except for the use of two small blockouts as spacers to back up the W-beam after the tubular W-beam terminated. Figure 14 shows the installation before Test 3.

A 4,595-pound Cadillac impacted the rail at 61.8 miles per

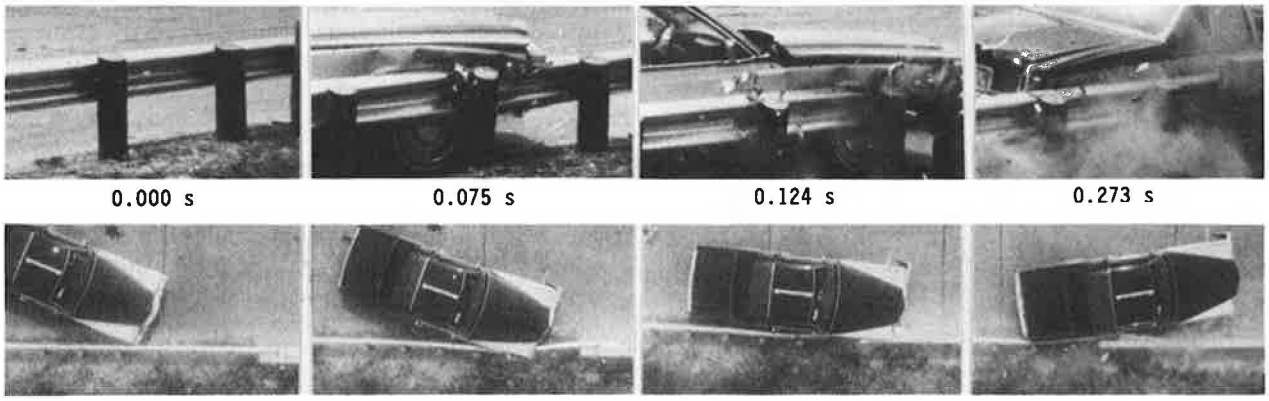

Test No	2461-2
Date	5/28/87
Test Installation	Tubular W-Beam Transition to T501
Length of Transition	25 ft (7.6 m)
Vehicle	1979 Cadillac
Vehicle Weight	
Test Inertia	4470 lb (1998 kg)
Gross Static	4637 lb (2075 kg)
Vehicle Damage Classification	
TAD	11LFQ5
CEC	01RYES3
Maximum Vehicle Crush	7.0 in (17.8 cm)
Max. Dyn. Rail Deflection	9.6 in (24.4 cm)
Max. Perm. Rail Deformation	6.0 in (12.2 cm)
Impact Speed	60.8 mi/h (97.8 km/h)
Impact Angle	25.8 deg
Exit Speed	41.4 mi/h (66.6 km/h)
Exit Angle	15.0 deg
Vehicle Accelerations (Max. 0.050-sec Avg)	
Longitudinal	-7.8 g
Lateral	-10.6 g
Occupant Impact Velocity	
Longitudinal	24.6 ft/s (7.5 m/s)
Lateral	24.1 ft/s (7.3 m/s)
Occupant Ridedown Accelerations	
Longitudinal	-2.9 g
Lateral	-13.8 g

FIGURE 13 Summary of results for Test 2.

FIGURE 14 W-beam to tubular W-beam transition, Test 3 installation.

FIGURE 15 Vehicle damage after Test 3.

hour and 24.2 degree, 125 inches upstream from the end of the tubular W-beam. Although significant wheel snagging was observed at several posts, the vehicle was safely redirected. The wheel snagging caused the post at the splice connection to separate from the rail and the next post downstream to splinter. This wheel snagging can be virtually eliminated through the use of rail-to-post blockouts in the transition region.

Vehicle damage was primarily concentrated in the area of the right front wheel, which snagged on a number of posts. Figure 15 shows vehicle damage after Test 3. Barrier damage after Test 3 is shown in Figure 16.

The exit angle and change in velocity of the test vehicle were above the recommended values of NCHRP Report 230 Evaluation Criteria I (*2*). Blockouts throughout the length of the transition should greatly improve overall performance and correct the deficiencies mentioned above. Although not required for evaluation of a transition, all of the occupant severity measures from Test 3 were within recommended lim-

FIGURE 16 Barrier damage after Test 3.

its set forth in NCHRP Report 230 (*2*). A summary of the test results is given in Figure 17.

DISCUSSION OF RESULTS

The tubular W-beam transition was judged to have met the intent of the performance criteria set forth in NCHRP Report 230 (*2*). The transition test is, first and foremost, a strength test. In this regard, the tubular W-beam transition has been shown to be able to contain and redirect a 4,500-pound vehicle impacting at a high speed and angle.

It is noted that for all three tests, the change in vehicle velocity exceeded the 15 miles per hour value recommended in NCHRP 230 Evaluation Criteria I (*2*). Although meeting this criteria is desirable, it is believed that strict compliance to this factor is not critical. This criteria is a subjective evaluation based on whether or not the vehicle is judged to have been redirected into or stopped while in adjacent traffic lanes. In all three crash tests described herein, the test vehicle returned to the side of the road after a short time interval and was not projected across traffic lanes. Depending on the existence and width of a shoulder, the test vehicles may or may not have briefly encroached on adjacent traffic lanes.

The primary intent of Evaluation Criteria I is to prevent the redirected vehicle from becoming a potential hazard to other traffic. It should be noted that, at this time, there is no definitive evidence that post impact trajectory is a serious problem. Further, impacting the transition at such a severe speed and angle is a low probability event. Although, as stated above, the change in vehicle velocity exceeded the recommended value of 15 miles per hour, the occupant impact velocities and ridedown accelerations were within maximum acceptable limits (*2*) for all three tests. This fact suggests that the severity of impact was well within tolerance limits.

NEW CONSTRUCTION TRANSITION DESIGN

It should be emphasized that the design that was crash tested is a retrofit of the existing Texas standard transition. The basic tubular W-beam design can be adapted for new construction applications by simply moving the entire single W-beam approach barrier 15 inches closer to the end of the concrete carrier. This adjustment will eliminate the need for a splice plate and will allow the single W-beam to be spliced directly onto the front rail of the tubular W-beam. Further, the posts upstream from the tubular W-beam (i.e., the posts to which the single W-beam approach rail is attached) can be offset 3 inches closer to the roadway. This will eliminate the need for the spacer blocks at the end of the single W-beam.

The modifications described above are intended to reduce the number of details in the transition design and, thereby, aid in the ease of field installation. Further changes can be implemented to improve the impact performance of the design. The exposed end of the concrete bridge rail may be beveled or flared. This should further reduce the possibility of wheel snag and could eliminate the need for the wood inserts used in Test 2. Finally, blockouts can be provided in the transition region. Blockouts would effectively eliminate wheel snagging on guardrail posts and should improve the overall impact performance of the barrier. A conceptual transition design that uses all of the above modifications is shown in Figure 18. Any or all of these variations may be used to improve upon the retrofit transition.

CONCLUSIONS AND RECOMMENDATIONS

A guardrail-to-bridge-rail transition from a W-beam to a rigid concrete barrier has been successfully designed and crash tested. A number of favorable characteristics have been incorporated into the design to help ensure acceptance and implementation in both retrofit and new construction applications. The tubular W-beam transition can easily retrofit existing installations, provides sufficient post spacing to allow implementation where bridge-end drains are required, and is designed for use with either a vertical concrete parapet or concrete safety-shaped barrier.

Although the change in vehicle velocity for these tests exceeded the recommended value of Evaluation Criteria I (*2*), it should be noted that the system that was tested is a

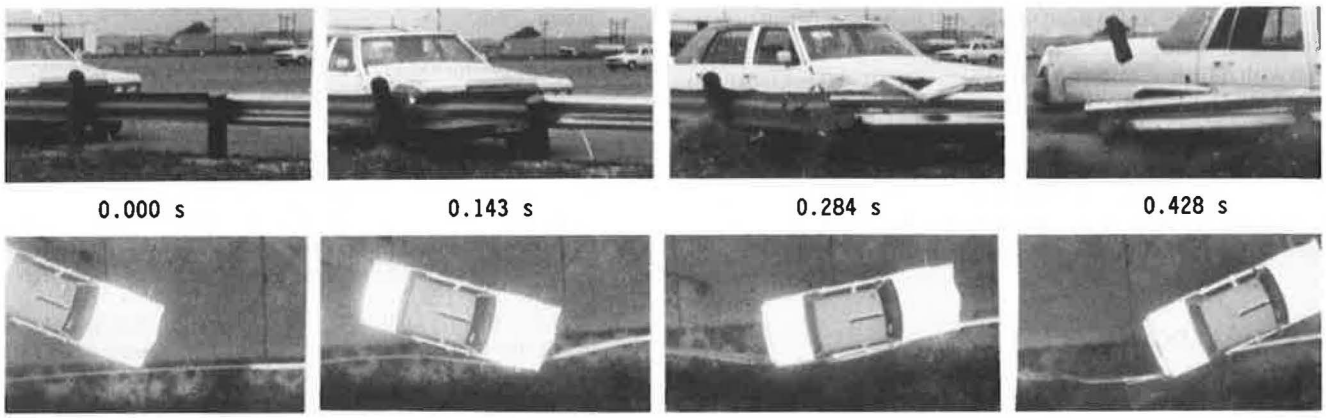

Test No	2461-3
Date	6/08/87
Test Installation	W-Beam Transition to Tubular W-Beam
Length of Transition	25 ft (7.6 m)
Vehicle	1979 Cadillac
Vehicle Weight	
Test Inertia	4430 lb (2011 kg)
Gross Static	4595 lb (2086 kg)
Vehicle Damage Classification	
TAD	11LFQ5
CEC	01RYES3
Maximum Vehicle Crush	12.0 in (30.5 cm)
Max. Dyn. Rail Deflection	2.6 in (0.8 cm)
Max. Perm. Rail Deformation	2.0 in (0.6 cm)
Impact Speed	61.8 mi/h (99.4 km/h)
Impact Angle	24.2 deg
Exit Speed	33.6 mi/h (54.1 km/h)
Exit Angle	18.1 deg
Vehicle Accelerations (Max. 0.050-sec Avg)	
Longitudinal	-6.2 g
Lateral	7.9 g
Occupant Impact Velocity	
Longitudinal	25.7 ft/s (7.8 m/s)
Lateral	17.4 ft/s (5.3 m/s)
Occupant Ridedown Accelerations	
Longitudinal	-10.1 g
Lateral	10.3 g

FIGURE 17 Summary of results for Test 3.

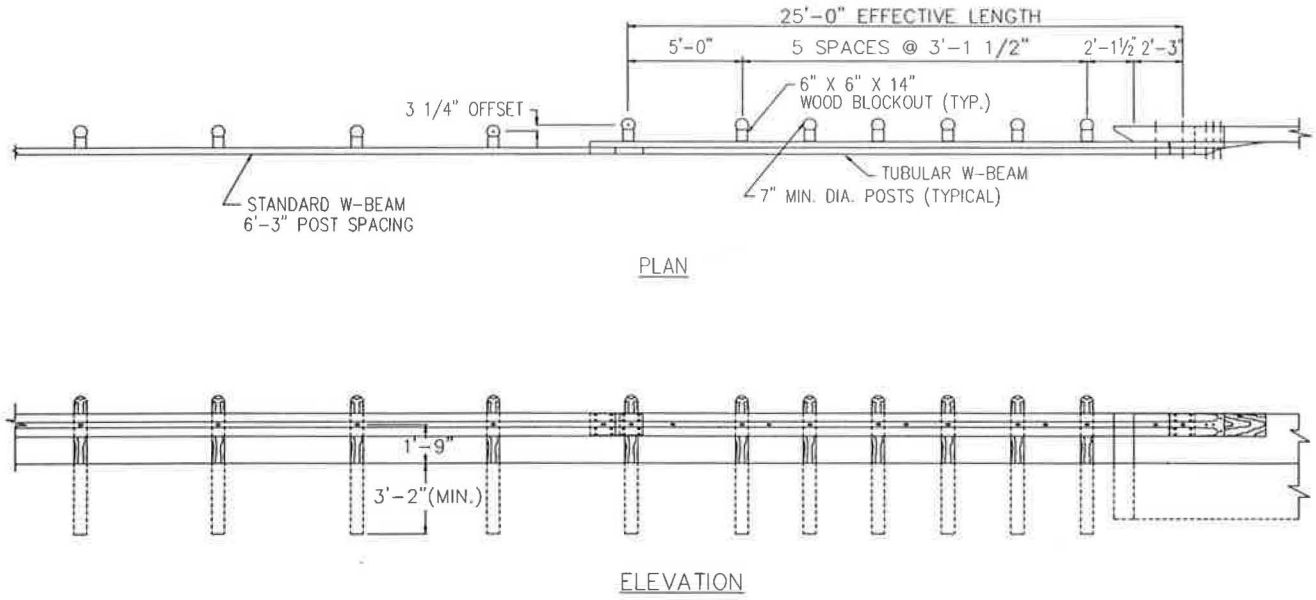

FIGURE 18 New construction transition.

retrofit design. To maintain compatibility with the standard Texas system, no blockouts were used. It is believed that the use of blockouts throughout the length of guardrail would eliminate post snagging.

Because of improved impact performance, it is recommended that the modified transition with wood inserts be used in conjunction with both the vertical parapet and safety-shaped barriers. The wood inserts are necessary to eliminate the propensity for the tubular beam to collapse.

For new construction applications it is recommended that the end of the concrete bridge rail be beveled or flared to reduce the potential for wheel snag. These modifications will

eliminate the need for wood reinforcement of the tubular W-beam. Although this system was developed for a 7-inch diameter round wood post, it is believed that it will perform equally well with 6-inch × 8-inch wood or W 6 × 9 steel posts because they have equivalent lateral strength characteristics.

The transition developed in this study greatly simplifies retrofit operations and offers designers an alternative for new construction projects. Based on the results of the full-scale testing, the tubular W-beam transition is suitable for immediate implementation for field evaluation.

ACKNOWLEDGMENTS

This research study was conducted under a cooperative program between the Texas Transportation Institute (TTI), the Texas State Department of Highways and Public Transportation (SDHPT), and the Federal Highway Administration (FHWA). John Panak, Harold Cooner, and Mark Marek of the SDHPT worked closely with the researchers and provided valuable input to this study. The authors are very appreciative of their comments and suggestions.

REFERENCES

1. M. E. Bronstad, L. R. Calcote, M. H. Ray, M. H., and J. B. Mayer. *Guardrail-Bridge Rail Transition Designs*. Report FHWA-RD-86-178, FWHA, U.S. Department of Transportation, 1986.
2. Jarvis D. Michie. *NCHRP Report 230: Recommended Procedures for the Safety Performance Evaluation of Highway Appurtenances*. TRB, National Research Council, Washington, D.C., 1981.
3. G. H. Powell. *A Computer Program for Evaluation of Automobile Barrier Systems*. Report No. FHWA-RD-73-51. FHWA, U.S. Department of Transportation, 1973.
4. H. E. Ross, Jr. Analysis and Design of Safety Appurtenances by Computer Simulation. *Proc., ASCE Specialty Conference on the Role of the Civil Engineer in Highway Safety*, New Orleans, La., 1983.
5. W. Lynn Beason et al. A Low-Maintenance, Energy-Absorbing Bridge Rail. In *Transportation Research Record 1065*, TRB, National Research Council, Washington, D.C., 1986.
6. L. R. Calcote. *Development of a Cost-Effectiveness Model for Guardrail Selection*. Southwest Research Institute Report 03-4309, FHWA contract DOT-FH-11-8827, Nov. 1977.
7. James F. Dewey, Jr., et al. *A Study of the Soil Structure Interaction Behavior of Highway Guardrail Posts*. Texas Transportation Institute Research Report 343-1, Texas A&M University, College Station, 1983.

gories. This would, for example, allow for determining the incremental effects of sideslopes of 2:1 or steeper, 3:1, 4:1, 5:1, 6:1, and 7:1 or flatter. The best sideslope model of this type was as follows:

$$AS = 731.16\ (0.839)^{W}\ (0.99995)^{ADT}\ (0.975)^{RECC}\ (0.909)^{SW} \times (1.373)^{SS1}\ (1.349)^{SS2}\ (1.238)^{SS3}\ (1.164)^{SS4}\ (1.091)^{SS5}$$

where

$SS1$ = 1 if sideslope = 2:1 or steeper, or zero otherwise,
$SS2$ = 1 if sideslope = 3:1, or zero otherwise,
$SS3$ = 1 if sideslope = 4:1, or zero otherwise,
$SS4$ = 1 if sideslope = 5:1, or zero otherwise,
$SS5$ = 1 if sideslope = 6:1, or zero otherwise.

For a sideslope of 7:1 or flatter, the last five terms of the equation would each become 1.0. For a sideslope of 2:1 or 1:1, the last four terms of the equation become 1.0 and the term $(1.373)^{SS1} = (1.373)^{1} = 1.373$, so the remaining terms of the equation are multiplied by a factor of 1.373. Likewise, for a sideslope of 3:1, the corresponding factor would be 1.349, and so on.

This model indicates that the rate of single-vehicle accidents decreases steadily for sideslope categories of 3:1, 4:1, . . . to 7:1 or flatter, as illustrated in figure 2. Figure 2 shows a ratio of the single-vehicle accident rate for a given sideslope to the single-vehicle accident rate for a sideslope of 7:1 or flatter. These values are based on the coefficients from the predictive model and using the 7:1 or flatter category as the basis of comparison. A review of figure 2 shows, for example, that the single-vehicle accident rate is 1.24 times higher on roads with a 4:1 sideslope than on roads with a sideslope of 7:1 or flatter. Note that little difference is found for sideslopes of 3:1, compared to those of 2:1 or steeper. This indicates that flattening sideslopes from 2:1 or steeper to 3:1 would be of little, if any, value in reducing single-vehicle accidents.

Based on the model results for various sideslopes, table 5 was developed to show likely reductions in single-vehicle accidents due to various sideslope flattening projects. Table 5 indicates that flattening a sideslope of 2:1 on a two-lane rural highway would be expected to reduce single-vehicle accidents by two percent if flattened to 3:1, 10 percent if flattened to 4:1, and 27 percent if flattened to 7:1 or flatter. Similarly, flattening a 4:1 sideslope to 7:1 or flatter would be expected to yield a 19 percent reduction in single-vehicle accidents.

The R^2 value for the above model was 0.19, which indicates that only 19 percent of the variation in the single-vehicle accident rate is explained by the variables in the model. While this may appear to be less than desirable, it should be remembered that high R^2 values rarely result from predictive modeling of accident experience, due to random accident fluctuations, imperfect accident reporting systems, effects of driver and vehicle factors on accidents, and other reasons. Also, accident rates tend to fluctuate widely, particularly on low volume roads.

In spite of the R^2 value, the model was found to be desirable in terms of reasonableness of the coefficients, significance of the model (at the 0.0001 level), inclusion of important variables (each of which had a significant effect on single-vehicle accidents), logical relationships between accidents and other variables, and reasonable predictive ability compared with real-world data.

Figure 3 shows the single-vehicle accident rate expected for six categories of sideslope and for 9-foot to 12-foot lane widths based on the predictive model. All curves are for sections with an ADT of 1,000, a shoulder width of 4 feet, and a 10-

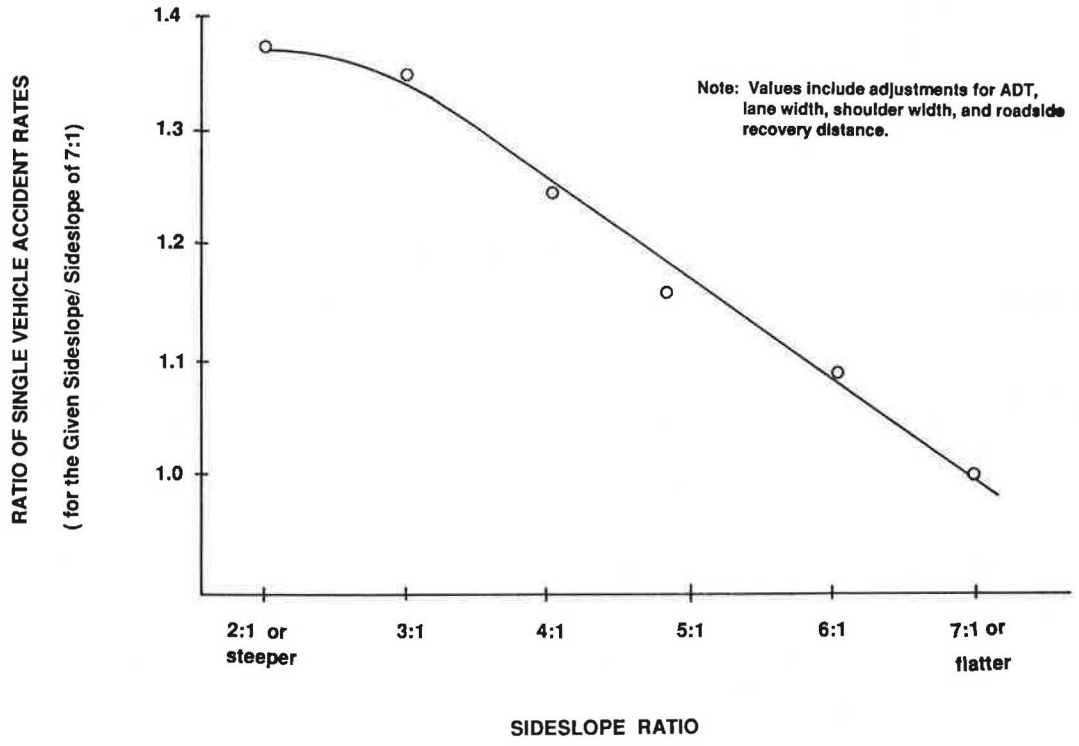

FIGURE 2 Plot of single-vehicle accident rate for a given sideslope versus single-vehicle accident rate for a sideslope of 7:1 or flatter.

TABLE 5 SUMMARY OF EXPECTED PERCENT REDUCTION IN SINGLE-VEHICLE ACCIDENTS DUE TO SIDESLOPE FLATTENING

Sideslope Ratio in Before Condition	Sideslope Ratio in After Condition				
	3:1	4:1	5:1	6:1	7:1 or Flatter
2:1	2	10	15	21	27
3:1	0	8	14	19	26
4:1	-	0	6	12	19
5:1	-	-	0	6	14
6:1	-	-	-	0	8

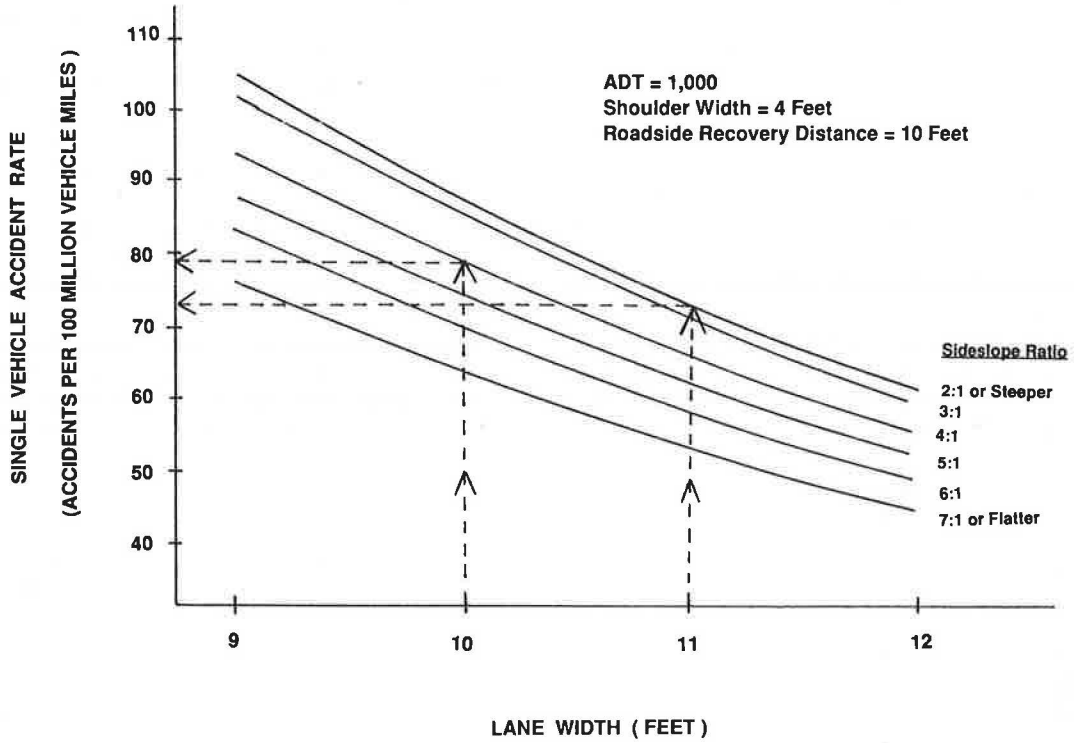

FIGURE 3 Illustration of single-vehicle accident rates for various lane widths and sideslopes.

foot roadside recovery distance beyond the shoulder edge. To illustrate the use of figure 3 for a lane width of 11 feet, sideslopes of 3:1, 4:1, and 6:1 would yield expected single-vehicle accident rates (accidents/100 mvm) of 72, 66, and 58, respectively.

The curves in figure 3 can also be used to determine trade-offs between the effects of lane width and sideslope. For example, for a roadway section with 1,000 ADT, 4-foot shoulders, 10-foot roadside recovery distance, 10-foot lane width, and a 4:1 sideslope, the expected single-vehicle accident rate is 79 (accidents/100 mvm). Widening this roadway to 11 feet would reduce the single-vehicle accident rate to 73, even if the resulting sideslopes were 2:1. Thus, in this example, one foot of lane widening at the expense of a steeper sideslope should not adversely affect the rate of single-vehicle accidents (although the overall accident severity may possibly be affected if, for example, more rollover accidents occur as a result of steepened sideslopes). While other types of comparisons can also be made using figure 3, the use of the predictive equation would allow for comparing the effects of sideslope changes on the single-vehicle accident rate versus lane and shoulder widening and roadside improvements.

Similar types of log-linear models were fitted using the rollover accident rate (AR) as the dependent variable. The best model for the rollover accident rate was

$$AR = 192.99\ (1.319)^{SS}(0.849)^{W}(0.983)^{RECC} \times (0.99984)^{ADT}(0.958)^{SW}$$

$$R^2 = .25$$

where

AR = rollover accidents per 100 million vehicle miles
SS = 1 if sideslope is 4:1 or steeper, or zero otherwise; all other terms are as previously defined.

This model has only two categories of sideslope, since no consistent trends were found in rollover rate for more defined sideslope groups. Note that in this model, a 4:1 sideslope was included with the steep (3:1 and 2:1 or steeper) group. This could indicate that sideslopes of 5:1 are more desirable than 4:1 slopes in preventing rollover accidents. Another explanation is that some vehicle types, such as mini-cars, are having a rollover accident problem on 4:1 sideslopes as well as on 3:1 and 2:1 slopes, which could partly account for the relatively high rollover accident rate for 4:1 sideslopes.

It should also be remembered that for each of the sample sections, the value of the sideslope used in the modeling was the 50th percentile (median value) of all of the field measurements for that section. A section labelled as having a 4:1 sideslope might actually consist of a range of sideslopes with 4:1 as the median value. Thus, in the database, each section labelled as 4:1 could have as much as 49 percent of the measurements steeper than 4:1 and the rest 4:1 or flatter. It is, therefore, quite possible that the 4:1 sideslope sections have rollover accident rates similar to the 3:1 and steeper category because these sections consist of a substantial portion of 3:1 and 2:1 sideslopes.

Rollover accidents represent only 23 percent of single-vehicle accidents (and only 8 percent of total accidents) in the database, so the relatively small samples of rollover accidents could have resulted in less reliable models than the models using single-vehicle accident rate. Also, the actual density of roadside fixed objects (such as trees) is generally greater on sections with steeper slopes than on sections with flat slopes. Thus, if a vehicle runs off the road onto the sideslope, it may hit an obstacle before having a chance to roll. Because of such considerations, it was believed that the rate of single-vehicle accidents was a better indication of sideslope effects than the rate of rollover accidents.

The single-vehicle accident model discussed earlier (and corresponding accident reductions) for various sideslopes provides perhaps the most reliable results currently available of sideslope effects on accidents. However, there remains considerable uncertainty relative to the precise rollover potential of various sideslopes (in conjunction with ditch types, height of fill, shoulder dropoff, etc.) for different vehicle characteristics.

Roadside Obstacle Types and Accidents

Another analysis involved determining the types of roadside obstacles that are most commonly struck on roads with various traffic volume conditions. The frequency of six types of fixed-object accidents for different ADT categories is summarized in table 6, based on data from six of the states in the current database. Utah accident data were not included because very few obstacle types were recorded in that state's accident file. Obstacle types other than trees, signs, utility poles, mailboxes, bridge ends, and guardrails were defined or recorded differently in different states, making tabulation of those types impossible.

Overall, the most frequently struck obstacles listed on table 6 were trees (14.8 percent) and utility poles (14.1 percent). This finding agrees with Jones and Baum (*10*) who cited these two obstacle types as among the most frequently struck fixed objects. Guardrail (9.6 percent), signs (6.5 percent), mailboxes (4.7 percent), and bridge ends (1.1 percent) were hit less frequently. The "other obstacle" category in table 6 includes all other obstacle types (including earth embankments) in addition to obstacles that were not specifically coded by the police officers.

For roads with ADTs of 4,000 or less, trees are the single most common type of obstacle struck. This may simply be the result of the fact that trees are generally the most common type of obstacle along low-volume rural roads. For roads with ADTs over 4,000, utility poles are the single most frequent type of fixed object struck, which is logical in view of the fact that higher volume roads are generally in the urban and suburban areas where utility poles are frequently placed near the roadway. Guardrail accidents accounted for less than seven

TABLE 6 FIXED-OBJECT ACCIDENTS BY ADT GROUP AND TYPE OF OBSTACLE STRUCK ON URBAN AND RURAL HIGHWAYS

ADT Group	Number of Accidents (Percent of accidents by ADT class)							
	Trees	Signs	Utility Poles	Mail Boxes	Bridge Ends	Guard Rail	Other Obstacles	Total FO Accs.
50-400	31(24.0)	6(4.7)	2(1.6)	2(1.6)	1(0.8)	5(3.9)	82(63.6)	129(100.0)
401-750	92(23.7)	20(5.2)	24(6.2)	10(2.6)	5(1.3)	20(5.2)	217(55.9)	388(100.0)
751-1,000	107(22.4)	9(1.9)	26(5.4)	6(1.3)	2(0.4)	33(6.9)	295(61.7)	478(100.0)
1,001-2,000	278(15.8)	95(5.4)	118(6.7)	46(2.6)	33(1.9)	192(10.9)	997(56.7)	1,759(100.0)
2,001-4,000	467(15.8)	200(6.8)	319(10.8)	144(4.9)	29(1.0)	319(10.8)	1,475(49.9)	2,953(100.0)
4,001-7,500	483(13.8)	235(6.7)	611(17.5)	198(5.7)	31(0.9)	323(9.3)	1,609(46.1)	3,490(100.0)
> 7,500	275(10.9)	198(7.9)	556(22.1)	145(5.8)	31(1.2)	239(9.5)	1,070(42.6)	2,514(100.0)
Total	1,733(14.8)	763(6.5)	1,656(14.1)	551(4.7)	132(1.1)	1,131(9.6)	5,745(49.1)	11,711(100.0)

Note: The data base includes 1,741 urban and rural sections in six states (excludes Utah).

percent of all fixed-object accidents on roads with ADTs of 1,000 or less, but they account for 9.3 to 10.9 percent of fixed-object hits for roads with ADTs of 1,001 or greater. The values in table 6 represent only the frequency of accidents and do not account for the placement or frequency (exposure) of these roadside objects.

It was impossible to determine the relative severity of accident types from the seven-state database, since data were aggregated by sections. However, accident data from the states of Michigan, Utah, and Washington were available for this analysis. These data include the rural two-lane roads, urban two-lane roads, and/or multi-lane roads. Nonetheless, the analysis afforded a reasonable look at the relative severity of different fixed-object (FO) accident types.

The severity of run-off-road fixed-object accidents relative to other common accident types was investigated, and the results are summarized in table 7. The percentage of FO accidents resulting in injury were 35, 36, and 44 for Michigan, Utah, and Washington, respectively. These percentages were lower than the percentages for rollover, head-on, and pedestrian/bicycle accidents; higher than the percentages for sideswipe opposite direction and sideswipe same direction; and about the same as the percentages for rear-end and angle accidents. The percentages of FO accidents resulting in a fatality were 0.8, 2.0, and 1.5 for Michigan, Utah, and Washington, respectively. These percentages again ranked FO accidents in the middle of the eight accident types shown in table 7. In terms of absolute numbers of injury accidents, however, FO accidents were the most frequent of the eight accident types in Michigan, the second most frequent in Washington, and the fourth most frequent in Utah. FO accidents were also the accident type most frequently associated with fatalities in Michigan and in Washington (fifth in Utah). In summary, FO accidents are both frequent and severe compared to other accident types.

The relative severity of the different types of fixed-object accidents is summarized by state in table 8. Fixed-object accidents which resulted in injuries generally ranged from 24 to 64 percent, depending on the type of object struck. Fatalities generally ranged from 0.2 to 6.1 percent. Among the objects associated with the highest percentage of injury and fatality were trees, culverts, bridges (bridge columns and bridge ends),

TABLE 7 SEVERITY OF COMMON ACCIDENT TYPES IN SEVERAL DATABASES

Accident Type	Accident Severity	Percent of accidents within type resulting in injury or fatality		
		State		
		Michigan	Utah	Washington
Run-off-road fixed object	Injury	35 (10137)	36 (827)	44 (15902)
	Fatal	0.8 (228)	2.0 (46)	1.5 (532)
Run-off-road rollover	Injury	55 (6587)	55 (1076)	56 (6488)
	Fatal	1.1 (73)	3.2 (63)	2.1 (245)
Head on	Injury	41 (1922)	50 (237)	60 (803)
	Fatal	2.7 (127)	11.9 (56)	20.4 (272)
Sideswipe Opposite dir.	Injury	21 (27)	30 (162)	41 (1118)
	Fatal	2.4 (3)	1.9 (10)	2.0 (54)
Sideswipe Same dir.	Injury	13 (42)	11 (87)	20 (2012)
	Fatal	1.6 (5)	0.2 (2)	0.2 (20)
Rear end	Injury	27 (2228)	33 (2320)	43 (21239)
	Fatal	0.3 (27)	0.2 (11)	0.2 (96)
Pedestrian or bicycle	Injury	86 (1769)	84 (654)	90 (2007)
	Fatal	7.0 (144)	7.8 (61)	9.8 (218)
Angle	Injury	46 (3145)	31 (2768)	37 (13272)
	Fatal	1.1 (78)	0.1 (55)	0.5 (174)

Note: The Michigan data base consisted of all reported accidents on rural roads in 1983. The Utah data base consisted of accidents reported from mid-1980 to mid-1985 on routes which had portions chosen as sections for the seven-state data base (and thus, included limited amounts of urban and multi-lane road accidents). The Washington data base consisted of all accidents reported in the State from 1980 through 1984.

( ) = The total numbers of accidents of the given type are in parenthesis.

TABLE 8 SEVERITY OF COMMON RUN-OFF-ROAD FIXED-OBJECT ACCIDENT TYPES IN SEVERAL DATA BASES

Accident Type	Accident Severity	Percent of total accidents resulting in injury or fatality		
		Data Base		
		Michigan	Utah	Washington
Utility/Light Pole	Injury	45 (3385)	39 (163)	47 (2282)
	Fatal	0.8 (58)	1.2 (5)	1.6 (75)
Guardrail	Injury	35 (1392)	42 (130)	41 (3403)
	Fatal	0.7 (28)	4.2 (13)	1.7 (144)
Sign	Injury	25 (1397)	24 (74)	40 (700)
	Fatal	0.4 (22)	1.3 (4)	1.4 (25)
Fence	Injury	28 (851)	35 (139)	40 (594)
	Fatal	0.2 (7)	1.0 (4)	1.7 (26)
Tree	Injury	47 (4419)		53 (984)
	Fatal	1.8 (171)		3.4 (64)
Culvert	Injury	49 (250)		64 (277)
	Fatal	3.3 (17)		2.1 (9)
Bridge Rail	Injury	41 (178)		41 (1060)
	Fatal	0.7 (3)		1.6 (42)
Bridge Column	Injury			54 (53)
	Fatal			6.1 (6)
Bridge End	Injury			53 (72)
	Fatal			5.2 (7)
Barrier Wall	Injury			41 (908)
	Fatal			0.5 (10)
Earth Embankment	Injury			53 (1793)
	Fatal			1.6 (55)
Rock	Injury			49 (891)
	Fatal			1.1 (21)
Mailbox	Injury			40 (132)
	Fatal			0.0 (0)
Fire Hydrant	Injury			30 (44)
	Fatal			0.7 (1)

Note: The Michigan data base consisted of all reported accidents on rural roads in 1983. The Utah data base consisted of accidents reported from mid-1980 to mid-1985 on routes which had portions chosen as sections for the seven-state data base (and thus, included limited amounts of urban and multi-lane road accidents). The Washington data base consisted of all accidents reported in the STate from 1980 through 1984.

( ) = The total numbers of accidents of the given type are in parenthesis.

rocks, utility poles, and earth embankments. Objects associated with the lowest percentages of injury and fatality were signs, mailboxes, fire hydrants, barrier walls, and fences. Trees, utility and light poles, guardrails, and earth embankments are the objects involved in the most FO injury and fatal accidents.

SUMMARY AND CONCLUSIONS

The purpose of this study was to determine the effects of various roadside features on accident experience. Detailed traffic, accident, roadway, and roadside data were collected on 4,951 miles of two-lane rural roads in seven states. Statistical analyses and log-linear modeling were used to determine the effects of various roadside and roadway features on single-vehicle and other related accident types. Roadside measures used in the analysis included a roadside hazard scale (a seven-point pictorial scale), the roadside recovery distance (clear zone distance), and field measurements of roadside side slope.

A reduction of one rating value on the seven-point roadside hazard scale (such as a five hazard rating to a four rating) due to a roadside improvement is estimated to result in a 19 percent reduction in related (AO) accidents. A 34 percent reduc-

tion in related accidents may be expected for a two-point reduction in hazard rating, a 47 percent reduction for a three-point decrease in roadside hazard rating, and a 52 percent accident reduction for a four-point decrease in hazard rating. Similar effects on accidents were found using a different predictive model when roadside recovery distance was increased. Reductions in related accidents were found to be 13 percent, 25 percent, 35 percent, and 44 percent, when the roadside recovery distance (as measured from the outside edge of shoulder to the nearest roadside obstacles or hazards) was increased on a section by an additional five feet, 10 feet, 15 feet, and 20 feet, respectively. These results were based on log-linear models that controlled for the effects of lane width, width of paved and unpaved shoulders, traffic volume, and terrain.

The effects of sideslope on accident experience were determined using a sample of 595 rural roadway sections (1,776 miles) in Alabama, Michigan, and Washington where field sideslope measurements were taken. Based on log-linear modeling that controlled for the effects of ADT, lane width, shoulder width, and roadside recovery distance, increased rates of single-vehicle accidents and rollover accidents were found for steeper sideslopes. The rate of single-vehicle accidents decreased steadily for sideslopes of 3:1 to 7:1 or flatter. However, only a slight reduction (2 percent) in single-vehicle accidents was found for a 3:1 sideslope compared to a sideslope of 2:1 or steeper. Expected reductions in single-vehicle accidents due to sideslope flattening ranged from 2 to 27 percent, depending on the sideslope in the before and after condition. For example, flattening sideslopes of 2:1 or steeper to 3:1, 4:1, 5:1, 6:1, or 7:1 or flatter would be expected to result in reductions in single-vehicle accidents of two percent, 10 percent, 15 percent, 21 percent, and 27 percent, respectively. Improvements to existing 3:1 sideslopes would reduce single-vehicle accidents by 8 percent, 19 percent, and 26 percent due to flattening them to 4:1, 6:1, and 7:1 or flatter, respectively.

Overall, trees and utility poles are the roadside fixed obstacles most often struck, while guardrails, signs, mailboxes, and bridge ends are less frequently struck. On roads with traffic volumes of 4,000 vehicles per day or less, trees are the obstacles most often struck, while utility poles are the obstacles most frequently struck on roadways with higher volumes. Roadside objects associated with the highest percentages of severe (injury plus fatal) accidents include culverts, trees, utility and light poles, bridges, rocks, and earth embankments, while signs, mailboxes, fire hydrants, barrier walls and fences were associated with lower percentages of severe accidents.

RECOMMENDATIONS

The results of this study clearly show the importance of roadside conditions on accidents for two-lane roads, and the safety effects of improving roadside conditions were quantified. It is recommended that highway agency officials use this information to determine where roadside improvements are justified. For example, on future 3R projects and highway reconstruction projects, the benefits of various roadside improvements should be determined using the information described in this paper. By estimating the costs for such roadside improvements such as sideslope flattening, removing trees, and relocating utility poles, the cost effectiveness may be determined.

Agencies could also consider the safety impacts of various roadside conditions when designing new highway segments, in order to minimize roadside hazards. Highway agencies should also be sensitive to highway sections where roadside improvements are feasible. In addition, when locations are identified which have an unusually high incidence of single-vehicle accidents, the accident reduction factors contained in this paper may be useful for computing expected accident benefits from roadside improvements and thus for weighing various project alternatives.

ACKNOWLEDGMENTS

This paper was based on joint study for the Federal Highway Administration and Transportation Research Board by Goodell-Grivas, Inc. The Highway Safety Research Center of the University of North Carolina served as a Subcontractor for the study. Appreciation is given to Justin True, the FHWA Contract Manager and John Deacon and Robert Skinner, who served as the TRB contract managers. Special thanks are also given to numerous state representatives in Alabama, Michigan, Montana, North Carolina, Utah, Washington, and West Virginia, who cooperated with the project team and provided necessary data and information. The field sideslope measurements used in the analysis were collected by Analysis Group, Inc., under a separate contract for FHWA. The authors assume responsibility for the accuracy of the information contained herein.

REFERENCES

1. S. A. Smith, J. Purdy, H. W. McGee, D. W. Harwood, A. D. St. John, and J. C. Glennon. *Identification, Quantification, and Structuring of Two-Lane Rural Highway Safety Problems and Solutions*. Volumes I and II, Report Nos. FHWA/RD/83/021 and 83/022, Federal Highway Administration, Washington, D.C., 1983.
2. C. V. Zegeer, J. G. Mayes, and R. C. Deen. *Cost-Effectiveness of Lane and Shoulder Widening of Rural, Two-Lane Roads in Kentucky*. Bureau of Highways, Kentucky Department of Transportation, 1979. Also in *Transportation Research Record 806*, TRB, National Research Council, Washington, D.C., 1981.
3. C. V. Zegeer, J. Hummer, L. Herf, D. Reinfurt, and W. Hunter. *Safety Effects of Cross-Section Design for Two-Lane Roads*. FHWA/RD/87/008, Federal Highway Administration, Washington, D.C., 1986.
4. F. D. Newcomb, and D. B. Negri. *Motor Vehicle Accidents Involving Collision with Fixed Objects*. New York State Department of Motor Vehicles, 1971.
5. E. A. Rinde. *Conventional Road Safety: Phase 1—A Study of Fixed Objects*. California Department of Transportation, 1979.
6. T. J. Foody and M. D. Long. *The Specification of Relationships Between Safety and Roadway Obstructions*. Report No. OHIO-DOT-06-74, Ohio Department of Transportation, 1974.
7. J. W. Hall, C. J. Burton, D. G. Coppage, and L. V. Dickinson. Roadside Hazards on Non-Freeway Facilities. In *Transportation Research Record 601*, TRB, National Research Council, Washington, D.C., 1976.
8. C. V. Zegeer and M. R. Parker. *Cost-Effectiveness of Coun-*

termeasures for Utility Pole Accidents. Report No. FHWA/RD/87/008, Federal Highway Administration, Washington, D.C., January 1983.
9. K. K. Mak and R. L. Mason. *Accident Analysis—Breakaway and Non-breakaway Poles Including Sign and Light Standards Along Highways*. Federal Highway Administration, Washington, D.C., 1980.
10. I. S. Jones and A. S. Baum. *An Analysis of the Urban Utility Pole Problem*. Federal Highway Administration, Washington, D.C., 1980.
11. J. L. Graham and D. W. Harwood. *NCHRP Report 247: Effectiveness of Clear Recovery Zones*. TRB, National Research Council, Washington, D.C., 1982.
12. J. D. Weaver and E. L. Marquis. Roadside Slope Design for Safety. *Transportation Engineering Journal*, American Society of Civil Engineers, 1976.
13. K. Perchonok, T. A. Ranney, S. Baum, D. F. Morrison, and J. D. Eppick. *Hazardous Effects of Highway Features and Roadside Objects*. Calspan Field Service, Inc., Federal Highway Administration, Washington, D.C., 1978.
14. L. Graf, J. U. Boos, and J. A. Wentworth. Single-Vehicle Accidents Involving Utility Poles. In *Transportation Research Record 571*, TRB, National Research Council, Washington, D.C., 1976, pp. 36–43.
15. T. C. Edwards, J. E. Martinez, W. F. McFarland, and H. E. Ross. *NCHRP Report 77: Development of Design Criteria for Safer Luminaire Supports*. HRB, National Research Council, Washington, D.C., 1968.
16. J. C. Glennon and C. J. Wilton. A Methodology for Determining the Safety Effectiveness of Improvements on All Classes of Highways. *Volume I: Effectiveness of Roadside Safety Improvements*. Report No. FHWA/RD/75/23, Federal Highway Administration, Washington, D.C., 1974.
17. D. E. Cleveland and R. Kitamura. Macroscopic Modeling of Two-Lane Rural Roadside Accidents. In *Transportation Research Record 681*, TRB, National Research Council, Washington, D.C., 1978.

Publication of this paper sponsored by Committee on Methodology for Evaluating Highway Improvements.